

MOL #65920

# **DIFFERENT N-TERMINAL MOTIFS DETERMINE PLASMA MEMBRANE TARGETING OF hCNT3 IN POLARIZED AND NON-POLARIZED CELLS**

Ekaitz Errasti-Murugarren, F. Javier Casado and Marçal Pastor-Anglada

Departament de Bioquímica i Biologia Molecular, Facultat de Biologia, Universitat de  
Barcelona.

IBUB - Institut de Biomedicina de la Universitat de Barcelona, Spain . CIBER EHD,  
Spain.

EE-M present address:

Institut de Recerca Biomèdica (IRB),  
Barcelona, Spain

MOL #65920

**Running title:** hCNT3 sorting and ER export

**Corresponding author address:** Marçal Pastor-Anglada, Ph.D. Departament de Bioquímica i Biologia Molecular. Facultat de Biologia. Universitat de Barcelona and CIBER EHD. Avda Diagonal 645. Edifici annex. Planta -1. 08028 Barcelona.

Tel. +34 93 402 1543 / 1544. Fax +34 93 402 1559. E-mail: [mpastor@ub.edu](mailto:mpastor@ub.edu)

**Number of text pages:** 37

**Number of tables:** 3 and 3 supplementary tables

**Number of figures:** 6

**Number of references:** 41

**Number of words in the *Abstract*:** 241

**Number of words in the *Introduction*:** 769

**Number of words in the *Discussion*:** 1265

**Abbreviations List:** hCNT, human concentrative nucleoside transporter; GFP, green fluorescent protein; DMEM, Dulbecco's modified eagle's medium; MDCK, Madin-Darby canine kidney cells; PBS, phosphate buffered saline.

MOL #65920

## ABSTRACT

hCNT3 is a broad selectivity high affinity concentrative nucleoside transporter protein implicated in the uptake of most nucleoside-derived anticancer and antiviral drugs. Regulated trafficking of hCNT3 has been recently postulated as a suitable way to improve nucleoside-based therapies (Fernandez-Calotti and Pastor-Anglada, 2010). Moreover, the recent identification of a putative novel hCNT3-type transporter lacking the first 69 amino acids and retained at the endoplasmic reticulum anticipated that the N-terminus of hCNT3 contains critical motifs implicated in trafficking (Errasti-Murugarren et al., 2009). In this study we have addressed this issue by using deletions and site-directed mutagenesis and plasma membrane expression and nucleoside uptake kinetic analysis. Data reveal that: 1) a segment between amino acids 50-62 contains plasma membrane sorting determinants in non-polarized cells; 2) in particular, the Val<sub>57</sub>-Thr<sub>58</sub>-Val<sub>59</sub> tripeptide appears to be the core of the export signal, whereas acidic motifs upstream and downstream of it seem to be important for the kinetics of the process; 3) in polarized epithelia the  $\beta$ -turn forming motif <sup>17</sup>VG<sup>20</sup>FQ is necessary for proper apical expression of the protein.

MOL #65920

## INTRODUCTION

Nucleosides play an important role as metabolic precursors in nucleic acid synthesis, being recycled through salvage pathways, and are crucial for the control of cell and tissue growth. In addition, many nucleoside analogues are currently used in anticancer and antiviral therapies, thus highlighting the pharmacological role these molecules can play in disease. Nucleoside-specific membrane transporters (NTs) mediate plasma membrane permeation of physiologic nucleosides and most nucleoside analogs, which will be further activated intracellularly by nucleoside kinases (Huber-Ruano and Pastor-Anglada, 2009; Molina-Arcas et al., 2009; Pastor-Anglada et al., 2008). Among these transporters, hCNT3 seems to play a crucial role in the disposition of physiological nucleosides and nucleoside analogs due to its broad substrate selectivity, high concentrative capacity and relatively wide tissue distribution (Errasti-Murugarren et al., 2009; Ritzel et al., 2001). In absorptive epithelia, apical localization of hCNT3 is crucial to determine vectorial flux of all antiviral and anticancer nucleosides tested so far (Errasti-Murugarren et al., 2007), thus being a major candidate to modulate drug pharmacokinetics. Interestingly, in Chronic Lymphocytic Leukemia (CLL) cells, hCNT3 protein is expressed but mostly in intracellular compartments, being its abundance a worse prognosis factor for time to disease progression (Mackey et al., 2005). Considering CLL patients are treated with fludarabine, a hCNT3 substrate, resistance to treatment could be partially due to impaired trafficking of hCNT3 into the plasma membrane of B cells. In this regard a recent report from our group showed that retinoic acid increases hCNT3 trafficking to the plasma membrane by a TGF- $\beta$ 1-dependent mechanisms in CLL-derived cell lines, which would eventually contribute to promote fludarabine-induced cytotoxicity (Fernandez-Calotti and Pastor-Anglada,

MOL #65920

2010). Despite the probable pharmacological relevance of nucleoside transporter trafficking mechanisms, this issue has been poorly addressed so far. In this regard, a previous study from our group reported that bile acids can increase plasma membrane CNT2-related activity by a short-term mechanism consistent with transporter recruitment from intracellular stores into the plasma membrane (Fernandez-Veledo et al., 2006).

Recently, a novel hCNT3-type transporter (hCNT3ins) has been identified. hCNT3ins lacks the first 69 amino acids of the cytoplasmic N-terminus, appears to be the result of alternative splicing of the *SLC28A3* gene and is retained intracellularly at the endoplasmic reticulum when expressed in non-polarized cells (Errasti-Murugarren et al., 2009). Expression in polarized MDCK cells also reveals a loss of fidelity for apical sorting (Errasti-Murugarren et al., 2009). These findings anticipate that the N-terminus of hCNT3 is implicated in protein trafficking in both polarized and non-polarized cells. In this regard, several classes of ER export signals in the cytoplasmic domains of proteins have been identified and include, for instance, two adjacent hydrophobic residues or diacidic motifs, although signals can also be conformational epitopes (Mancias and Goldberg, 2007; Nishimura and Balch, 1997; Otte and Barlowe, 2002; Votsmeier and Gallwitz, 2001; Zuzarte et al., 2007).

Unveiling the constitutive and regulated trafficking mechanisms of hCNT-type proteins, thereby controlling cell surface expression of these drug transporters might help to better understand how the uptake of natural nucleosides and clinically relevant nucleoside analogs is short-term regulated. As a first step in this goal and based upon the evidence obtained when analyzing hCNT3ins localization, in the present study we

MOL #65920

have constructed a series of truncated and mutated hCNT3 proteins to identify targeting motifs implicated in transporter sorting, both in polarized and non-polarized cells. In fact, a novel 13-mer comprising two putative diacidic motifs with a region in the middle with alternated hydrophilic and hydrophobic amino acids, has been identified as a key determinant of plasma membrane sorting and ER export in non-polarized cells. Interestingly, an additional motif, a tetrapeptide which may adopt a beta turn secondary structure has also been identified as a molecular determinant for apical sorting of hCNT3 in polarized MDCK cells. These experiments provide novel information about the residues that contribute to the protein localization and ER export suggesting as well the evidence that key differences exist in sorting mechanisms between polarized and non-polarized cells.

MOL #65920

## MATERIALS AND METHODS

**Reagents:** Uridine ([5,6-<sup>3</sup>H], 35-50 Ci/mmol) was purchased from Amersham Biosciences (UK). Uridine was obtained from Sigma-Aldrich (Saint Louis, MO, USA).

**Construction of GFP-fused mutants of human Concentrative Nucleoside Transporter 3 (hCNT3) cDNA:** Wild type human CNT3 cDNA was subcloned into the green fluorescent protein (GFP) vector, pEGFPC1/N1 (Clontech, Palo Alto, CA) as described previously (Errasti-Murugarren et al., 2007). The truncated hCNT3-pEGFP constructs were generated using the specific primer combinations defined in Table I and II (Supplementary Material) under PCR conditions outlined previously (Errasti-Murugarren et al., 2008). PCR products and the pEGFP vector were double-digested with Pst I and Hind III, the products were gel-isolated and ligated together to generate in-frame fusion proteins with enhanced green fluorescent protein (GFP) fused to the N or C terminus of each construct. The QuickChange<sup>TM</sup> site-directed mutagenesis kit (Stratagene, La Jolla, CA, USA) was used to generate hCNT3 sorting signal mutants according to the manufacturer's protocol. The GFP-fused hCNT3 chimera was used as template. Specific primer sequences are shown in Table III (Supplementary Material). All constructions were verified by DNA sequencing and used for transient transfection.

**Cell culture and transfection:** HeLa cells were maintained at 37°C/5%CO<sub>2</sub> in DMEM (BioWhittaker) supplemented with 10% fetal bovine serum (v/v), 50 units/ml penicillin, 50 µg/ml streptomycin and 2 mM L-glutamine. HeLa cells were transiently transfected with plasmid constructions mentioned above using Lipofectamine 2000 (Invitrogen, Carlsbad, CA, USA) following manufacturer's protocol. Nucleoside

MOL #65920

transport, confocal microscopy and flow cytometry analysis were carried out 24, 48 and 72 hours after transfection. MDCK cells were also maintained at 37°C/5%CO<sub>2</sub> in DMEM (BioWhittaker) supplemented with 10% fetal bovine serum (v/v), 50 units/ml penicillin, 50 µg/ml streptomycin and 2 mM L-glutamine. Cells were plated in transwell plates (Corning Costar, Cambridge, MA, USA; 3402; 12 mm diameter, 0.3 µm pore) and transfected as previously described (Harris et al., 2004).

***Nucleoside transport assay:*** Nucleoside uptake was measured as described previously (del Santo et al., 1998) by exposing replicate cultures at room temperature to [<sup>3</sup>H]-labeled uridine (1 µM, 1 µCi/ml, Amersham Pharmacia Biotech) in sodium or sodium-free transport buffer (137 mM NaCl or 137 mM choline chloride, 5 mM KCl, 2 mM CaCl<sub>2</sub>, 1 mM MgSO<sub>4</sub>, 10 mM HEPES, pH 7.4). Initial rates of transport were determined using an incubation period of 1 minute. Assays were terminated by washing with an excess volume of chilled buffer. Saturation kinetics was evaluated by non-linear regression analysis and the kinetic parameters derived from this method were confirmed by linear regression analysis of the derived Eadie-Hofstee plots.

***Transwell transport experiments:*** The transwell filter inserts were washed three times with sodium or sodium-free buffer, and then 1 µM [<sup>3</sup>H]-uridine (Amersham Pharmacia Biotech) was added to the apical or basal side. Transport experiments were conducted with buffer (0.5 ml in the apical compartment and 0.5 ml in the basal compartment) containing sodium or choline on both sides of the Transwell filters. The transport experiments were terminated by aspirating the buffer, and filters were washed with chilled buffer. The whole filter was wiped with tissue to remove any excess of



MOL #65920

buffer, the filter was removed from the plastic support and counted on a scintillation counter. The cells on the filters were solubilised using 0.1 % SDS 100 mM NaOH.

***Visualization of nucleoside transporters tagged with green fluorescent protein:***

To analyze the effect of the mutations on plasma membrane sorting of hCNT3, confocal microscopy of GFP-fused chimeras was performed on a semi-confluent monolayer of transfected HeLa cells cultured on glass coverslips. Glass coverslips-grown cells were rinsed three times with phosphate-buffered saline- $\text{Ca}^{2+}$ - $\text{Mg}^{2+}$ , fixed for 15 minutes in PFA 3% sucrose 0.06 M, and rinsed three times with phosphate-buffered saline, and then mounted with aqua-poly/mount coverslipping medium (Polysciences, Inc. Warrington, PA). Endoplasmic reticulum retention was analyzed by co-transfecting GFP-fused transporter chimeras with pDsRed2-ER (BD Living Colors). Sections were viewed using a Leica TCS SP5 laser scanning confocal microscope (Leica Microsystems Heidelberg GmbH, Mannheim, Germany) equipped with a DMI6000 inverted microscope, argon laser, diode-pumped solid-state (561 nm), and a 63x oil immersion objective lens (NA 1.4) was used. For visualization of GFP and pDsRed2-ER labellings, images were acquired sequentially using 488 and 561 nm laser lines, AOBS as beam splitter, emission detection ranges 500-550, 571-650 nm, respectively, and the confocal pinhole set at 1 airy units. Optical sections were collected every 0.3 microns in a 1024 x 1024 format, zoom 4 and pixel size 60 nm x 60 nm. Transfection efficiency as well as fluorescence intensity were determined by flow cytometry using a Cytomics FC 500 MPL Flow Cytometry System (Beckman Coulter).

To analyze the polarized membrane sorting of GFP-fused hCNT3 and hCNT3 mutants,  $1.7 \times 10^5$  MDCK cells were grown in twelve-well Corning Costar

MOL #65920

polycarbonate transwell filter inserts for 24 hours and then transfected as explained previously. The filters were rinsed three times with phosphate-buffered- $\text{Ca}^{2+}$ - $\text{Mg}^{2+}$ , fixed for 15 minutes in PFA 3% sucrose 0.06 M, excised and then loaded on a glass slide and covered with a coverslip. Between the slide and the coverslip, a ~1 mm gap was filled with aqua-poly/mount coverslipping medium (Polysciences, Inc. Warrington, PA). Actin was stained using phalloidin-TRITC (Sigma-Aldrich, Saint Louis, MO, USA). Images were also obtained using a Leica TCS SP5 laser scanning confocal microscope (Leica Microsystems Heidelberg GmbH, Mannheim, Germany). Optical sections were collected every 0.3 microns in a 1024 x 1024 format, zoom 4 and pixel size 60 nm x 60 nm.

**Data Analysis:** Data are expressed as the mean  $\pm$  s.d. of uptake values obtained in three wells or filter inserts. Data are representative of three experiments carried out on different days on different batches of cells.

MOL #65920

## RESULTS

*Deletion of the cytoplasmic N-terminus of hCNT3 causes ER retention in a non-polarized cell model.* To gain insight into the signal sequence(s) required for targeting of hCNT3 to the plasma membrane in a non-polarized cell model, we employed a truncation approach, in which the full-length protein was progressively shortened from the N-terminus. hCNT3 mutants fused to the N- or C-terminus of the GFP were generated, transiently expressed in HeLa cell line and the subcellular distribution and kinetic properties of each truncation mutant were determined 24 hours after transient transfection. HeLa cells were transfected with the plasmids coding for the wild-type GFP-hCNT3, GFP-hCNT3 $\Delta$ 35, GFP-hCNT3 $\Delta$ 49, GFP-hCNT3 $\Delta$ 58, GFP-hCNT3 $\Delta$ 62 or GFP (Fig. 1). Functional characterization of these constructions resulted in a significant sodium-dependent uridine transport activity for the wild-type and the 35 and 49 amino acid-deleted mutants, whereas GFP-hCNT3 $\Delta$ 62 expressing HeLa cells did not show any sodium-dependent uridine transport activity. On the other hand the GFP-hCNT3 $\Delta$ 58 construction showed a slightly higher uridine sodium-dependent activity than that shown by HeLa cells transfected with the GFP vector (Fig. 1B). Confocal microscopy analysis of transfected HeLa cells showed that truncation of 35 and 49 amino acids had no effect on plasma membrane sorting whereas truncation of 62 amino acids resulted in ER retention of the transporter. The deletion of 58 amino acids resulted in both ER retention and little but significant plasma membrane localization (Fig. 1C). The intracellular localization of these chimeras was determined by co-transfection of GFP-fused hCNT3 truncation mutants with pDsRed2-ER, a specific marker of the ER. As shown in figure 1C, wild type hCNT3 and 35 and 49 amino acids truncated mutants did not co-localize with the ER marker, being mainly expressed at the cell surface,

MOL #65920

whereas the 62 amino acids truncated mutant and most but not all of the 58 amino acids deleted mutant showed a distribution pattern coincident with the ER marker. Moreover, flow cytometry analysis revealed similar transfection rates for all constructions but slight differences in fluorescence intensity values (Table 1). Kinetic analysis of the plasma membrane expressed mutants showed no differences in uridine affinity (Supplementary Fig. 1), which suggests that the N-terminus of the transporter is not involved in substrate specificity. The calculation of  $V_{max}$ /fluorescence intensity ratios for each construction corroborated proper membrane sorting for both the 35 and 49 amino acids truncated constructions and intracellular retention of the 58 amino acid truncation (Table 1). In all cases results were identical with the N1- or C1GFP-fused chimeras (data not shown).

***A 13-residue long peptide of the hCNT3 N-terminus is involved in the ER export and plasma membrane sorting in a non-polarized cell model.*** These results demonstrate that amino acids between 50 and 62 are important for cell surface targeting. This 13-residue long peptide comprised two acidic motifs (residues <sup>53</sup>DEE<sup>55</sup> and <sup>60</sup>EQD<sup>62</sup> of the human CNT3 sequence) with a region in the middle with alternated hydrophilic and hydrophobic amino acids (residues <sup>56</sup>QVTV<sup>59</sup>). These motifs are conserved in the N-terminus of the concentrative nucleoside transporter 3 from several species (Fig. 2A). To identify further the potential role of these domains in the export of CNT3 protein from the ER, we generated a series of mutants in which each amino acid of the sequence <sup>50</sup>TKQDEEQVTVEQD<sup>62</sup> was substituted by an alanine individually or in combination (Fig. 2B). Wild type and hCNT3 mutants conjugated with GFP were transiently expressed in HeLa cells and their activities and subcellular localization were revealed by uptake assays and confocal microscopy, respectively (Fig. 2B and C).

MOL #65920

Individual mutation of residues Tyr<sub>50</sub>, Lys<sub>51</sub>, Gln<sub>52</sub>, Asp<sub>53</sub>, Glu<sub>54</sub>, Glu<sub>55</sub>, Gln<sub>56</sub>, Gln<sub>61</sub> or Asp<sub>62</sub> did not significantly influence the activity and subcellular localization of hCNT3 mutants after a 24 hours culture (Fig. 2B and C). In contrast, single mutations of Val<sub>57</sub>, Thr<sub>58</sub>, Val<sub>59</sub> and Glu<sub>60</sub> abolished transporter activity and were associated with intracellular ER retention (Fig. 2B, C and D). Nevertheless, the sodium-dependent uridine transport measured 48 hours after transfection reached similar values to those observed for the wild type construction (Supplementary Fig. 2A). In this regard, analysis of the activity and subcellular localization 48 hours after transfection revealed a clearly distinguishable plasma membrane localization of the mutants (Supplementary Fig. 2B), suggesting that these mutations did not completely block but rather slowed down the delivery of hCNT3 to the plasma membrane. Substitution of Val<sub>57</sub> and/or Val<sub>59</sub> with isoleucine had no effect on transporter activity and subcellular localization (data not shown). Because the presence of acidic motifs has been suggested to be essential for cell-surface expression of several plasma membrane proteins (Nishimura and Balch, 1997; Votsmeier and Gallwitz, 2001; Zuzarte et al., 2007), we determined the effect of either double or triple mutations of Asp<sub>53</sub>-Glu<sub>55</sub> on hCNT3 activity and subcellular localization. Our results indicate that, although individual mutation of Asp<sub>53</sub>, Glu<sub>54</sub> or Glu<sub>55</sub> had no obvious effect on transporter export from ER, double and triple mutations of acidic residues to alanine resulted in intracellular ER retention and dramatic loss of plasma membrane sodium-dependent uridine transport activity (Fig. 2B and C). In this case, these changes also appeared to be the result of slow trafficking, because proper sodium-dependent uridine uptake and plasma membrane localization were revealed 48 hours after transfection (Supplementary Fig. 2A and B). However, mutation of tripeptide Val<sub>57</sub>-Thr<sub>58</sub>-Val<sub>59</sub> to Ala<sub>57</sub>-Ala<sub>58</sub>-Ala<sub>59</sub> resulted in a complete retention of the transporter in the ER even at 72 hours after transfection (Supplementary

MOL #65920

Fig. 2A and B). This observation suggests that these amino acids are the core of the hCNT3 ER export signal and that the acidic motifs upstream and downstream this core region are important for the kinetics of the sorting process. Results were identical in all cases with either the N1GFP- or the C1GFP-fused chimeras (data not shown).

***The cytoplasmic N-terminus of hCNT3 contains an apical targeting signal.*** As introduced above, CNT type proteins show an asymmetrical distribution in polarized cells, being present at the apical surface and determining vectorial flux of nucleosides (Errasti-Murugarren et al., 2007; Ngo et al., 2001). Since deletion of the first 69 amino acids from the N-terminus of hCNT3 results in missorting of the transporter protein in polarized cells (Errasti-Murugarren et al., 2009), a series of truncation mutants were also generated to define the specific requirements for normal apical localization of hCNT3. Polarized MDCK cells were transfected with the plasmids coding for GFP-fused hCNT3, hCNT3 $\Delta$ 10, hCNT3 $\Delta$ 25, hCNT3 $\Delta$ 69 or GFP. The steady-state membrane distribution of these mutants was determined by activity assays on polarized MDCK cells grown on transwell inserts (Fig. 3B) and confirmed using immunofluorescence confocal microscopy of fixed monolayers (Fig. 3C). These data confirmed that hCNT3 was present in the apical domain of polarized MDCK. Deletion of the first 10 amino acids from the N-terminus of hCNT3 had no effect on transporter apical sorting, whereas deletion of either 25 or 69 amino acids resulted in a similar missorting of hCNT3. In fact, both deleted constructs resulted in a significant reduction of the apical and a concomitant increase of the basolateral sodium-dependent uridine transport (Fig. 3B). Moreover, flow cytometry analysis showed the same transfection rates but different fluorescence intensity values for all constructions (Table 2), being the hCNT3 truncated mutant activities corrected by their fluorescence intensities (Table 3).

MOL #65920

Altogether, these data identified a sequence of 15 amino acids (<sup>11</sup>AEGYSNVGFQNEENF<sup>25</sup>) which appears to be important for polarized expression of hCNT3 in MDCK cells. In all cases results were identical with either the N1GFP- or the C1GFP-fused chimeras (data not shown).

*A tetrapeptide adopting a  $\beta$ -turn structure is implicated in apical sorting of hCNT3.* The analysis of the 15-residue long peptide sequence showed no evident structural motifs, apart from a clustering of negatively charged amino acids in the distal part of the sequence. The alignment of this amino acid sequence with the equivalent one from different CNT3 orthologs showed a low conservation degree among different species (Fig. 4A). Several short cytosolic motifs have been identified as positive apical sorting or ER export signals in polarized models. Among these, Sun *et al* defined a fourteen amino acid sequence required for optimal apical membrane targeting of the rat ileal bile acid transporter, with a beta turn tetramer within this sequence sufficient to produce an apical bias of protein location (Sun et al., 2003). On the basis of this report, we analyzed the conformational topology of these selected 15 amino acids of the hCNT3 N-terminus applying a predictive method to identify beta turns within proteins named tetrapeptide residue-coupled model, developed by Chou in 1997 (Chou, 1997). Using this method successive tetrapeptide regions along the N-terminal region of hCNT3 were analyzed for propensity to form beta turns, scored in terms of a discriminant function delta, where values > 0 indicate the tetrapeptide forms a beta turn. Within the 15-amino acids long peptide identified using the truncation approach of the cytoplasmic N-terminus of hCNT3 we found one tetrapeptide that scored positively for the occurrence of a beta turn (<sup>17</sup>VGFQ<sup>20</sup>) (Fig. 4C). Similar beta turn forming tetrapeptides were found within the corresponding 15-residue long peptide of some but

MOL #65920

not all of the orthologs analyzed, suggesting a common mechanisms of apical sorting for some CNT3 orthologs (Fig. 4C). In addition, substitution of the putative cytosolic beta turn domain with a similar but non-beta turn forming tetrapeptide (MTFR) (Chou, 1997) resulted in a similar phenotype to that previously observed for the deletion of 25 and 69 amino acids, with a reduction in the apical and an increase in the basolateral sodium-dependent uridine transport activity (Fig. 4B). The steady-state membrane distribution of these mutants was confirmed using immunofluorescence confocal microscopy of fixed monolayers (Fig. 4D). Moreover, flow cytometry analysis showed similar transfection rates and fluorescence intensity values for all constructions. hCNT3 mutant activities were corrected by their fluorescence intensities to allow better comparisons (Table 3). In all cases results were identical with the N1- or C1GFP-fused chimeras (data not shown).



MOL #65920

## DISCUSSION

In the present contribution, N-terminus truncated mutants of hCNT3 have been used to reveal: 1) that the N-t was not implicated in substrate binding, which is in agreement with previous data (Hamilton et al., 2001; Loewen et al., 1999) and 2) that a 13-residues long peptide between amino acids 50-62 contained plasma membrane sorting determinants in non-polarized cell models. Alanine scanning mutagenesis of this region revealed the presence of two different domains essential for proper plasma membrane sorting of the transporter, a PDZ binding domain type II-like sequence and negatively charged amino acids upstream and downstream this core region. This particular amino acid distribution is highly conserved in all CNT3 orthologs, suggesting a common mechanism for CNT3 protein sorting in non-polarized cell models. Individual mutations of <sup>57</sup>VTV<sup>59</sup> to alanines resulted in intracellular ER-derived structures retention of hCNT3 transporter mutants 24 hours after transfection. One possible explanation of these structures is that vesicles budding from ER and containing hCNT3 mutants leave ER and fuse homotypically to give rise to larger containers, as described for GAT1 mutants (Farhan et al., 2008). However, in contrast to those described for GAT1 mutants, these ER-derived structures are not a dead-end for hCNT3 mutants as they are able to reach the plasma membrane 48 hours post-transfection. Additionally, mutation of <sup>57</sup>VTV<sup>59</sup> to <sup>57</sup>AAA<sup>59</sup> resulted in ER retention of the mutant, suggesting an essential role for this domain in the ER export of the hCNT3 transporter.

Replacement of either V<sub>57</sub> or V<sub>59</sub> with other non-polar amino acids, similar to those found in other orthologs, resulted in fully active hCNT3 transporter showing that it was the hydrophobic nature of valine that leads to efficient ER export. The

MOL #65920

importance of hydrophobic residue-based sorting signals has been described in the interaction of transmembrane cargo with COPII components (Otte and Barlowe, 2002) as well as in protein-protein interactions occurring at the plasma membrane. In this regard, three different PDZ domain recognition motifs (classes I-III) depending on valine residues play a role in protein transport to the plasma membrane (Nourry et al., 2003). In addition to the valine, these motifs require a critical amino acid at position -2; in class II a hydrophobic residue at position -2 (XΨXΨ) in the peptide interacts with a corresponding hydrophobic residue in the PDZ containing protein (Nourry et al., 2003). In the case of hCNT3 the valine residue in position -2 is also essential for ER export, being likely that this internal <sup>56</sup>QVTV<sup>59</sup> motif of the transporter is recognized during ER export by PDZ domain containing proteins. Moreover, the role of this sequence in COPII dependent ER export could not be excluded; a possibility that warrants further studies.

Furthermore our experiments ruled out the importance of diacidic motifs in hCNT3 ER export. In fact, residues <sup>53</sup>DEE<sup>55</sup> and <sup>60</sup>EQD<sup>62</sup> might confer the consensus of the ER export diacidic motif (DE/X/ED). This motif is present in the cytoplasmic tail of several transmembrane proteins (Nishimura et al., 1999; Votsmeier and Gallwitz, 2001; Zuzarte et al., 2007). Individual mutations of negatively charged amino acids from both putative diacidic motifs resulted in fully functional transporters, except for the mutation E60A, which showed an ER-derived structures intracellular retention, as showed for previous hCNT3 mutants. The progressive substitution of negatively charged amino acids by alanines produced a decrease in surface expression and in transport activity of the CNT3 transporter, suggesting the need of at least two negatively charged amino acids preceding the <sup>56</sup>QVTV<sup>59</sup> domain, as well as the Glu<sub>60</sub> downstream this domain for

MOL #65920

transporter export from the ER. This result is in accordance with previous reports showing that the immediate environment of certain motifs affect their function (Mancias and Goldberg, 2007), thus suggesting a role for the acidic residues referred to above in the maintenance of the proper spatial conformation of the <sup>56</sup>QVTV<sup>59</sup> domain. Nevertheless, an additional role for these acidic residues besides the structural one cannot be ruled out.

hCNT3 is also expressed in a variety of epithelia in which its apical sorting and expression might determine vectorial flux of nucleosides and nucleoside-derived drugs (Damaraju et al., 2007; Errasti-Murugarren et al., 2007; Mangravite et al., 2003). In fact, in contrast to basolateral sorting motifs, the interaction of apical sorting determinants of proteins with the sorting machinery of polarized cells is still poorly understood. The known motifs identified so far are highly diverse, often consisting of posttranslational modifications or transmembrane domains which enable preferential association of the protein with plasma membrane microdomains, being not as strict as prototypical basolateral determinants (Ellis et al., 2006). Moreover, several short cytosolic motifs have been identified as positive apical sorting or ER export signals in polarized models (Francesconi and Duvoisin, 2002; Karim-Jimenez et al., 2000; Kwon and Guggino, 2004; Sun et al., 2003). In fact, non-conserved amino acid sequences in different protein orthologs might define by themselves structural signals for ER export and polarized sorting (Subramanian et al., 2004; Sun et al., 2004; Sun et al., 2003). In this study we showed that the efficient arrival of hCNT3 to the apical domain of the polarized MDCK cell model requires four amino acids (<sup>17</sup>VGFQ<sup>20</sup>) in the proximal segment of the cytosolic amino terminus. The prediction of the secondary structure of the proximal segment of the N-terminus of hCNT3 indicated that a potential turn

MOL #65920

structure may occur between amino acids 17 and 20. In this regard,  $\beta$ -turn forming peptides have been proposed as being implicated in either basolateral or apical sorting (Aroeti et al., 1993; Subramanian et al., 2004; Sun et al., 2004; Sun et al., 2003). Disruption of this probable  $\beta$ -turn structure by either deletion or site-directed mutagenesis to form a non- $\beta$ -turn tetrapeptide, resulted in partial missorting of hCNT3 from the apical to the basolateral domain, either during secretion or after endocytosis, as described for CFTR (Moyer et al., 1999). Although the probability of  $\beta$ -turn structure is apparently not conserved in a few orthologs, when their primary sequences were analyzed based upon the tetrapeptide residue-coupled model (Chou, 1997), this does not fully rule out its occurrence. In fact, our data show that this apical sorting signal is necessary but not sufficient to confer polarized apical localization of hCNT3 in MDCK cells. In this regard, some membrane proteins contain multiple sorting signal motifs that are regulated by several sorting factors and mechanisms (Pei et al., 2000; Saunders and Limbird, 1997) suggesting the requirement of complementary signals for proper apical sorting of the hCNT3 transporter.

Understanding mechanisms responsible for hCNT3 trafficking may be of biological and pharmacological relevance. hCNT3 is found mostly in intracellular stores in CLL cells and this occurrence associates with poor prognosis in patients under fludarabine treatment (Mackey et al., 2005; Tsang et al., 2008). We recently found that hCNT3 trafficking into the plasma membrane can be stimulated in CLL but also in solid tumor derived cell lines by retinoic acid. This phenomenon is mediated by TGF- $\beta$ 1 and dependent upon the small GTPase RhoA (Fernandez-Calotti and Pastor-Anglada, 2010). Interestingly, Rho family members are found in vesicular compartments where they can

MOL #65920

play major roles in vesicle trafficking in both endocytic and exocytic pathways (Ridley, 2001; Symons and Rusk, 2003).

In summary, mapping of the N-terminus tail of the hCNT3 protein revealed that acidic and hydrophobic motifs in this domain control ER export and cell surface expression levels in non-polarized cells, whereas a putative  $\beta$ -turn domain contributes to hCNT3 polarized surface expression in epithelial cells. This represents a first step in the understanding of the mechanisms of constitutive and regulated hCNT3 trafficking, which is a relevant goal not only for a better understanding of hCNT3 biology, but also in the clinical treatment with nucleoside-derived drugs.

## ACKNOWLEDGEMENTS

We would like to express our gratitude to the Confocal Microscopy Facility of Serveis Científicotècnics (Universitat de Barcelona-IDIBAPS) for their support and advice with confocal techniques. We also thank I. Iglesias for technical assistance.

MOL #65920

## REFERENCES

- Aroeti B, Kosen PA, Kuntz ID, Cohen FE and Mostov KE (1993) Mutational and secondary structural analysis of the basolateral sorting signal of the polymeric immunoglobulin receptor. *J Cell Biol* **123**(5):1149-1160.
- Chou KC (1997) Prediction of beta-turns. *J Pept Res* **49**(2):120-144.
- Damaraju VL, Elwi AN, Hunter C, Carpenter P, Santos C, Barron GM, Sun X, Baldwin SA, Young JD, Mackey JR, Sawyer MB and Cass CE (2007) Localization of broadly selective equilibrative and concentrative nucleoside transporters, hENT1 and hCNT3, in human kidney. *Am J Physiol Renal Physiol* **293**(1):F200-211.
- del Santo B, Valdes R, Mata J, Felipe A, Casado FJ and Pastor-Anglada M (1998) Differential expression and regulation of nucleoside transport systems in rat liver parenchymal and hepatoma cells. *Hepatology* **28**(6):1504-1511.
- Ellis MA, Potter BA, Cresawn KO and Weisz OA (2006) Polarized biosynthetic traffic in renal epithelial cells: sorting, sorting, everywhere. *Am J Physiol Renal Physiol* **291**(4):F707-713.
- Errasti-Murugarren E, Cano-Soldado P, Pastor-Anglada M and Casado FJ (2008) Functional characterization of a nucleoside-derived drug transporter variant (hCNT3C602R) showing altered sodium-binding capacity. *Mol Pharmacol* **73**(2):379-386.
- Errasti-Murugarren E, Molina-Arcas M, Casado FJ and Pastor-Anglada M (2009) A splice variant of the SLC28A3 gene encodes a novel human concentrative nucleoside transporter-3 (hCNT3) protein localized in the endoplasmic reticulum. *Faseb J* **23**(1):172-182.
- Errasti-Murugarren E, Pastor-Anglada M and Casado FJ (2007) Role of CNT3 in the transepithelial flux of nucleosides and nucleoside-derived drugs. *J Physiol* **582**(Pt 3):1249-1260.
- Farhan H, Reiterer V, Kriz A, Hauri HP, Pavelka M, Sitte HH and Freissmuth M (2008) Signal-dependent export of GABA transporter 1 from the ER-Golgi intermediate compartment is specified by a C-terminal motif. *J Cell Sci* **121**(Pt 6):753-761.
- Fernandez-Calotti P and Pastor-Anglada M (2010) All-trans retinoic acid promotes trafficking of human concentrative nucleoside transporter-3 (hCNT3) to the plasma membrane by a TGF- $\beta$ 1-mediated mechanism. *J Biol Chem*.
- Fernandez-Veledo S, Huber-Ruano I, Aymerich I, Duflot S, Casado FJ and Pastor-Anglada M (2006) Bile acids alter the subcellular localization of CNT2 (concentrative nucleoside cotransporter) and increase CNT2-related transport activity in liver parenchymal cells. *Biochem J* **395**(2):337-344.
- Francesconi A and Duvoisin RM (2002) Alternative splicing unmasks dendritic and axonal targeting signals in metabotropic glutamate receptor 1. *J Neurosci* **22**(6):2196-2205.
- Hamilton SR, Yao SY, Ingram JC, Hadden DA, Ritzel MW, Gallagher MP, Henderson PJ, Cass CE, Young JD and Baldwin SA (2001) Subcellular distribution and membrane topology of the mammalian concentrative Na<sup>+</sup>-nucleoside cotransporter rCNT1. *J Biol Chem* **276**(30):27981-27988.
- Harris MJ, Kagawa T, Dawson PA and Arias IM (2004) Taurocholate transport by hepatic and intestinal bile acid transporters is independent of FIC1 overexpression in Madin-Darby canine kidney cells. *J Gastroenterol Hepatol* **19**(7):819-825.

MOL #65920

- Huber-Ruano I and Pastor-Anglada M (2009) Transport of nucleoside analogs across the plasma membrane: a clue to understanding drug-induced cytotoxicity. *Curr Drug Metab* **10**(4):347-358.
- Karim-Jimenez Z, Hernando N, Biber J and Murer H (2000) Requirement of a leucine residue for (apical) membrane expression of type IIb NaPi cotransporters. *Proc Natl Acad Sci U S A* **97**(6):2916-2921.
- Kwon SH and Guggino WB (2004) Multiple sequences in the C terminus of MaxiK channels are involved in expression, movement to the cell surface, and apical localization. *Proc Natl Acad Sci U S A* **101**(42):15237-15242.
- Loewen SK, Ng AM, Yao SY, Cass CE, Baldwin SA and Young JD (1999) Identification of amino acid residues responsible for the pyrimidine and purine nucleoside specificities of human concentrative Na(+) nucleoside cotransporters hCNT1 and hCNT2. *J Biol Chem* **274**(35):24475-24484.
- Mackey JR, Galmarini CM, Graham KA, Joy AA, Delmer A, Dabbagh L, Glubrecht D, Jewell LD, Lai R, Lang T, Hanson J, Young JD, Merle-Beral H, Binet JL, Cass CE and Dumontet C (2005) Quantitative analysis of nucleoside transporter and metabolism gene expression in chronic lymphocytic leukemia (CLL): identification of fludarabine-sensitive and -insensitive populations. *Blood* **105**(2):767-774.
- Mancias JD and Goldberg J (2007) The transport signal on Sec22 for packaging into COPII-coated vesicles is a conformational epitope. *Mol Cell* **26**(3):403-414.
- Mangravite LM, Badagnani I and Giacomini KM (2003) Nucleoside transporters in the disposition and targeting of nucleoside analogs in the kidney. *Eur J Pharmacol* **479**(1-3):269-281.
- Molina-Arcas M, Casado FJ and Pastor-Anglada M (2009) Nucleoside Transporter Proteins. *Curr Vasc Pharmacol*.
- Moyer BD, Denton J, Karlson KH, Reynolds D, Wang S, Mickle JE, Milewski M, Cutting GR, Guggino WB, Li M and Stanton BA (1999) A PDZ-interacting domain in CFTR is an apical membrane polarization signal. *J Clin Invest* **104**(10):1353-1361.
- Ngo LY, Patil SD and Unadkat JD (2001) Ontogenic and longitudinal activity of Na(+)-nucleoside transporters in the human intestine. *Am J Physiol Gastrointest Liver Physiol* **280**(3):G475-481.
- Nishimura N and Balch WE (1997) A di-acidic signal required for selective export from the endoplasmic reticulum. *Science* **277**(5325):556-558.
- Nishimura N, Bannykh S, Slabough S, Matteson J, Altschuler Y, Hahn K and Balch WE (1999) A di-acidic (DXE) code directs concentration of cargo during export from the endoplasmic reticulum. *J Biol Chem* **274**(22):15937-15946.
- Nourry C, Grant SG and Borg JP (2003) PDZ domain proteins: plug and play! *Sci STKE* **2003**(179):RE7.
- Otte S and Barlowe C (2002) The Erv41p-Erv46p complex: multiple export signals are required in trans for COPII-dependent transport from the ER. *Embo J* **21**(22):6095-6104.
- Pastor-Anglada M, Cano-Soldado P, Errasti-Murugarren E and Casado FJ (2008) SLC28 genes and concentrative nucleoside transporter (CNT) proteins. *Xenobiotica* **38**(7-8):972-994.
- Pei D, Kang T and Qi H (2000) Cysteine array matrix metalloproteinase (CA-MMP)/MMP-23 is a type II transmembrane matrix metalloproteinase regulated by a single cleavage for both secretion and activation. *J Biol Chem* **275**(43):33988-33997.

MOL #65920

- Ridley AJ (2001) Rho proteins: linking signaling with membrane trafficking. *Traffic* **2**(5):303-310.
- Ritzel MW, Ng AM, Yao SY, Graham K, Loewen SK, Smith KM, Ritzel RG, Mowles DA, Carpenter P, Chen XZ, Karpinski E, Hyde RJ, Baldwin SA, Cass CE and Young JD (2001) Molecular identification and characterization of novel human and mouse concentrative Na<sup>+</sup>-nucleoside cotransporter proteins (hCNT3 and mCNT3) broadly selective for purine and pyrimidine nucleosides (system cib). *J Biol Chem* **276**(4):2914-2927.
- Saunders C and Limbird LE (1997) Disruption of microtubules reveals two independent apical targeting mechanisms for G-protein-coupled receptors in polarized renal epithelial cells. *J Biol Chem* **272**(30):19035-19045.
- Subramanian VS, Marchant JS, Boulware MJ and Said HM (2004) A C-terminal region dictates the apical plasma membrane targeting of the human sodium-dependent vitamin C transporter-1 in polarized epithelia. *J Biol Chem* **279**(26):27719-27728.
- Sun AQ, Balasubramanian N, Liu CJ, Shahid M and Suchy FJ (2004) Association of the 16-kDa subunit c of vacuolar proton pump with the ileal Na<sup>+</sup>-dependent bile acid transporter: protein-protein interaction and intracellular trafficking. *J Biol Chem* **279**(16):16295-16300.
- Sun AQ, Salkar R, Sachchidanand, Xu S, Zeng L, Zhou MM and Suchy FJ (2003) A 14-amino acid sequence with a beta-turn structure is required for apical membrane sorting of the rat ileal bile acid transporter. *J Biol Chem* **278**(6):4000-4009.
- Symons M and Rusk N (2003) Control of vesicular trafficking by Rho GTPases. *Curr Biol* **13**(10):R409-418.
- Tsang RY, Santos C, Ghosh S, Dabbagh L, King K, Young J, Cass CE, Mackey JR and Lai R (2008) Immunohistochemistry for human concentrative nucleoside transporter 3 protein predicts fludarabine sensitivity in chronic lymphocytic leukemia. *Mod Pathol* **21**(11):1387-1393.
- Votsmeier C and Gallwitz D (2001) An acidic sequence of a putative yeast Golgi membrane protein binds COPII and facilitates ER export. *Embo J* **20**(23):6742-6750.
- Zuzarte M, Rinne S, Schlichthorl G, Schubert A, Daut J and Preisig-Muller R (2007) A di-acidic sequence motif enhances the surface expression of the potassium channel TASK-3. *Traffic* **8**(8):1093-1100.



MOL #65920

## FOOTNOTES

This research was supported in part by grants SAF2008-00577, CIBER (an initiative of Instituto de Salud Carlos III), 2009SGR624 (Generalitat de Catalunya) and BFU2006-07556/BFI.

Please send reprint requests to: Marçal Pastor-Anglada, Ph.D. Departament de Bioquímica i Biologia Molecular. Facultat de Biologia. Universitat de Barcelona and CIBER EHD. Avda Diagonal 645. Edifici annex. Planta - 1. 08028 Barcelona.

Tlf. +34 93 402 1543 / 1544.

Fax +34 93 402 1559.

E-mail: [mpastor@ub.edu](mailto:mpastor@ub.edu)

MOL #65920

## FIGURE LEGENDS

**Figure 1. Summary of the mutations made in the N-terminus of hCNT3 and their effects on plasma membrane expression and activity in HeLa cells.** A) Schematic representation of the N-terminus of hCNT3 (residues 1-102) and truncation mutants. B) Sodium-dependent uptake of [<sup>3</sup>H]-uridine (1 μM, 1 minute) by GFP-hCNT3 and GFP-fused truncation mutants was measured in transport medium containing 137 mM NaCl or 137 mM choline chloride. Sodium-dependent transport was calculated as uptake in NaCl medium minus uptake in choline chloride. Data are expressed as the mean ± s.d. of three experiments carried out on different days on different batches of cells. C) Subcellular localization of GFP-fused hCNT3 truncation mutants in HeLa cells compared to that of the full length GFP-hCNT3 protein (691 amino acids). Wild type hCNT3 and truncation mutants hCNT3Δ35 and hCNT3Δ49 are expressed at the plasma membrane, showing no overlapping with pDsRed2-ER expression, a protein expressed in the endoplasmic reticulum. On the other hand, truncation mutant hCNT3Δ62 co-localizes with pDsRed2-ER staining, indicating that this mutant is retained in the endoplasmic reticulum. Deletion of first 58 amino acids from N-terminus of hCNT3 (hCNT3Δ58) resulted in an intermediate pattern with both ER and plasma membrane being stained.

**Figure 2. An N-terminal motif dictates plasma membrane sorting in HeLa cells.** A) Primary structure of human CNT3 (residues 50-62). The amino acid sequence of human CNT3 (hCNT3, GenBank<sup>TM</sup> accession number AF305210) is compared with that of chimpanzee (ptCNT3, Ensembl<sup>TM</sup> accession number ENSDNOP00000046380), gorilla (goCNT3, Ensembl<sup>TM</sup> accession number ENSDNOP00000001197), orangutan

MOL #65920

(ppCNT3, Ensembl<sup>TM</sup> accession number ENSDNOP00000021660), pika (opCNT3, Ensembl<sup>TM</sup> accession number ENSDNOP00000003345), megabat (pvCNT3, Ensembl<sup>TM</sup> accession number ENSDNOP00000006777), mouse lemur (miCNT3, Ensembl<sup>TM</sup> accession number ENSDNOP00000009061), bushbaby (ogCNT3, Ensembl<sup>TM</sup> accession number ENSDNOP00000002294), dolphin (ttCNT3, Ensembl<sup>TM</sup> accession number ENSDNOP00000004747), cow (btCNT3, Ensembl<sup>TM</sup> accession number ENSBTAP00000024328), squirrel (stCNT3, Ensembl<sup>TM</sup> accession number ENSSTOP00000014307), guinea pig (cpCNT3, Ensembl<sup>TM</sup> accession number ENSCPOP00000011872), armadillo (dnCNT3, Ensembl<sup>TM</sup> accession number ENSDNOP00000003788), mouse (mCNT3, GenBank<sup>TM</sup> accession number AF305211), rat (rCNT3, GenBank<sup>TM</sup> accession number AY059414) and dog (cfCNT3, Ensembl<sup>TM</sup> accession number ENSDNOP00000001980). Suggested important domains are boxed. B) Sodium-dependent uptake of [<sup>3</sup>H]-uridine (1  $\mu$ M, 1 minute) by GFP-hCNT3 and GFP-fused alanine substitution mutants was measured as in Figure 1. Suggested important domain is boxed. Data are expressed as the mean  $\pm$  s.d. of three experiments carried out on different days on different batches of cells. C) Subcellular localization of wild type GFP-hCNT3 and GFP-fused alanine substitution mutants in HeLa cells. Wild type hCNT3 and mutants hCNT3T50A, K51A, Q52A, D53A, E54A, E55A, Q56A, Q61A and D62A are expressed at the plasma membrane, showing no overlapping with ER marker pDsRed2-ER. On the other hand, hCNT3V57A, T58A, V59A, <sup>53</sup>DE<sup>54</sup>/AA and <sup>53</sup>DEE<sup>55</sup>/AAA mutants were retained in intracellular ER derived structures. Finally, hCNT3<sup>57</sup>VTV<sup>59</sup>/AAA mutant co-localizes with pDsRed2-ER staining, indicating that this mutant is retained in the endoplasmic reticulum. D) Detailed intracellular ER derived structure from mutant hCNT3T58A and its colocalization with ER marker pDsRed2-ER.

MOL #65920

**Figure 3. Summary of the mutations made in the N-terminus of hCNT3 and their effects on plasma membrane expression and activity in MDCK cells.** A) Schematic representation of the N-terminus of hCNT3 (residues 1-102) and truncation mutants. B) Apical and basal sodium-dependent uptake of [<sup>3</sup>H]-uridine (1 μM, 1 minute) by GFP-hCNT3 and GFP-fused truncation mutants was measured in transport medium containing 137 mM NaCl or 137 mM choline chloride. Sodium-dependent transport was calculated as uptake in NaCl medium minus uptake in choline chloride. Data are expressed as the mean ± s.d. of three experiments carried out on different days on different batches of cells. C) Transiently transfected MDCK cells with GFP-tagged hCNT3, hCNT3 truncation mutants or vector alone. Cells were fixed, stained for actin with Texas Red<sup>TM</sup> conjugated phalloidin and visualized by confocal microscopy. Red, actin; Green, GFP. Subcellular localization of hCNT3 truncation mutants in MDCK cells was compared to that of the full length hCNT3 protein (691 amino acids). Wild type hCNT3 and truncation mutant hCNT3Δ10 are sorted to the apical plasma membrane, showing no basolateral staining. On the other hand, truncation mutants hCNT3Δ25 and Δ69 showed both apical and basolateral staining.

**Figure 4. An N-terminal motif dictates apical sorting of hCNT3.** A) Primary structure of human CNT3 (residues 11-25). The amino acid sequence of human CNT3 (hCNT3) is compared with that of chimpanzee (ptCNT3), orangutan (ppCNT3), cow (btCNT3), dog (cfCNT3), dolphin (ttCNT3), mouse lemur (miCNT3), megabat (pvCNT3), pika (opCNT3), squirrel (stCNT3), mouse (mCNT3) and rat (rCNT3). Protein accession numbers are the same as in Figure 2. Suggested β-turn forming tetrapeptide is boxed. B) Apical and basal sodium-dependent uptake of [<sup>3</sup>H]-uridine (1

MOL #65920

$\mu\text{M}$ , 1 minute) by hCNT3 and mutants was measured as in Figure 3. Data are expressed as the mean  $\pm$  s.d. of three experiments carried out on different days on different batches of cells. C) Application of tetrapeptide residue-coupled model (Chou, 1997) to predict the localization of  $\beta$ -turns within the putative N-terminal targeting region of hCNT3. Sequential tetrapeptides were assigned a  $\beta$ -turn attribute function ( $\Delta$ ), where the criterion for  $\beta$ -turn prediction is  $\Delta > 0$ . Prediction of occurrence of  $\beta$ -turns in N-terminal of hCNT3 (residues 11-25) (upper) and hCNT3 orthologs (lower). D) Transiently transfected MDCK cells with GFP-tagged hCNT3 and hCNT3 mutants. Cells were fixed, stained for actin with Texas Red<sup>TM</sup> conjugated phalloidin and visualized by confocal microscopy. Red, actin; Green, GFP. Subcellular localization of hCNT3 mutants in MDCK cells was compared to that of the full length hCNT3 protein (691 amino acids). Wild type hCNT3 is sorted to the apical plasma membrane, showing no basolateral staining, whereas the non- $\beta$ -turn forming hCNT3<sup>17</sup>VGFAQ<sup>20</sup>MTFR mutant showed both apical and basolateral staining.

MOL #65920

Construction	% Transfection	S.D.	Fluorescence Intensity (F.I.)	S.D.	Ratio $V_{max}/F.I.$
hCNT3	77.9	5.1	223.4	17	2.1
hCNT3Δ35	81.9	3.9	129.5	9.5	1.9
hCNT3Δ49	82.2	2.2	196.7	4.1	2.1
hCNT3Δ58	79.9	3.7	188.4	7.3	0.3

**Table 1. Transfection efficiency and fluorescence intensity of GFP-fused chimeras.**

HeLa cells were transfected with the GFP-fused chimeras and after 24 hours cells were resuspended and analyzed by flow cytometry for transfection efficiency and construction expression rate. The calculated  $V_{max}$  values obtained from Supplementary Figure 2 were normalized to the fluorescence intensity values. Fluorescence intensity is expressed as arbitrary units. Data are expressed as the mean  $\pm$  s.d. of three experiments carried out on different days on different batches of cells.

MOL #65920

Construction	% Transfection	S.D.	Fluorescence Intensity (F.I.)	S.D.
hCNT3	39.6	0.5	60.3	4.1
hCNT3Δ10	36.4	0.3	61.1	2.9
hCNT3Δ25	36.8	0.5	64.0	0.3
hCNT3Δ69	38.5	0.3	11.0	4.4
hCNT3 <sup>17</sup> VGfQ <sup>20</sup> MTFR	38.2	0.3	62.2	4.1

**Table 2. Transfection efficiency and fluorescence intensity of GFP-fused chimeras.**

MDCK cells were transfected with the GFP-fused chimeras and after 48 hours cells were resuspended and analyzed by flow cytometry for transfection efficiency and construction expression rate. Fluorescence intensity is expressed as arbitrary units. Data are expressed as the mean  $\pm$  s.d. of three experiments carried out on different days on different batches of cells.

MOL #65920

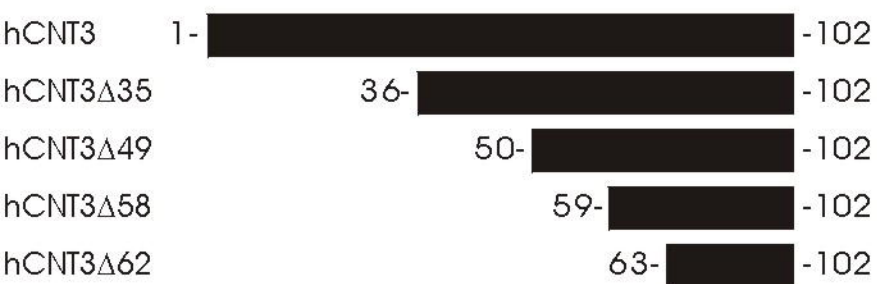
Construction	Apical activity	Basolateral activity	Ratio apical activity/F.I.	Ratio basolateral activity/F.I.	Ratio apical/basolateral
hCNT3	37.5 ± 3.6	3.5 ± 1.2	0.62	0.06	10.3
hCNT3Δ10	37.1 ± 0.7	3.6 ± 0.5	0.60	0.06	10.0
hCNT3Δ25	17.2 ± 0.7	6.9 ± 1.9	0.27	0.11	2.45
hCNT3Δ69	2.9 ± 0.3	1.0 ± 0.2	0.26	0.10	2.60
hCNT3 <sup>17</sup> VGFQ <sup>20</sup> MTFR	16.8 ± 0.8	7.2 ± 0.8	0.27	0.12	2.25

**Table 3. Analysis of the polarized sorting of GFP-fused chimeras.** MDCK cells were transfected with the GFP-fused chimeras and uridine uptake at both apical and basolateral domains was analyzed. GFP-fused transporters sodium-dependent uridine uptake was normalized by fluorescence intensity values from Table 2 and then the ratio between apical and basolateral uridine uptake was calculated. Uridine uptake was expressed as pmol/mg prot·min. Data are expressed as the mean ± s.d. of three experiments carried out on different days on different batches of cells.

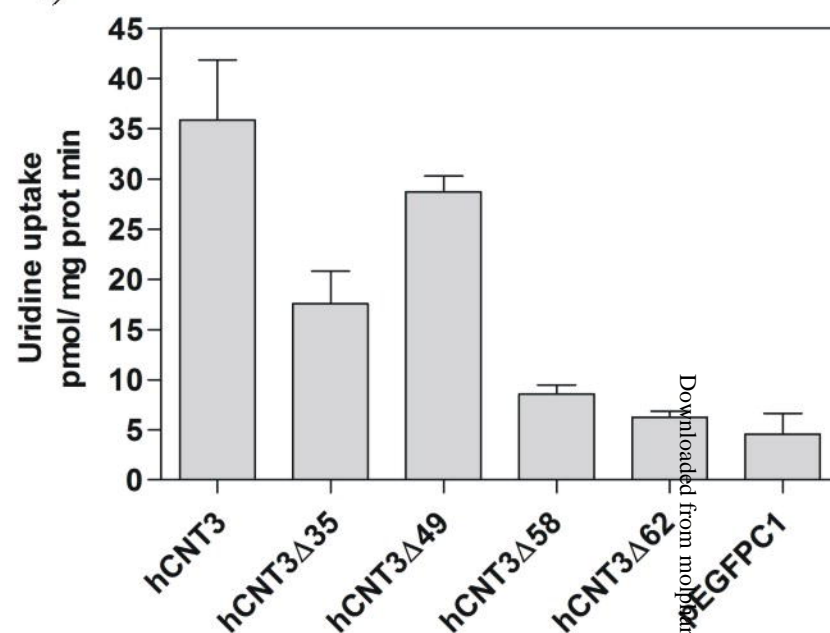


# Figure 1

A)



B)



C)

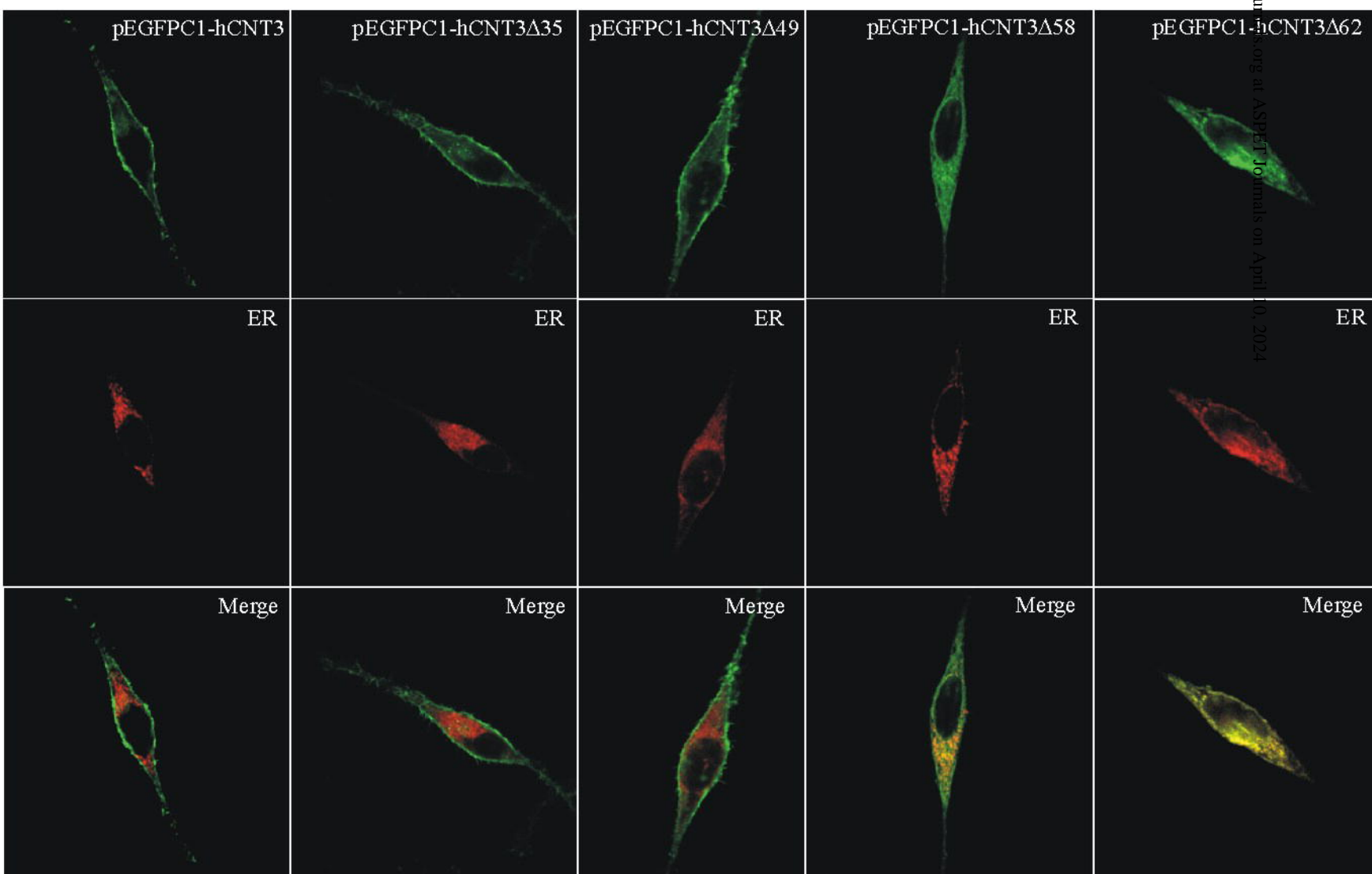


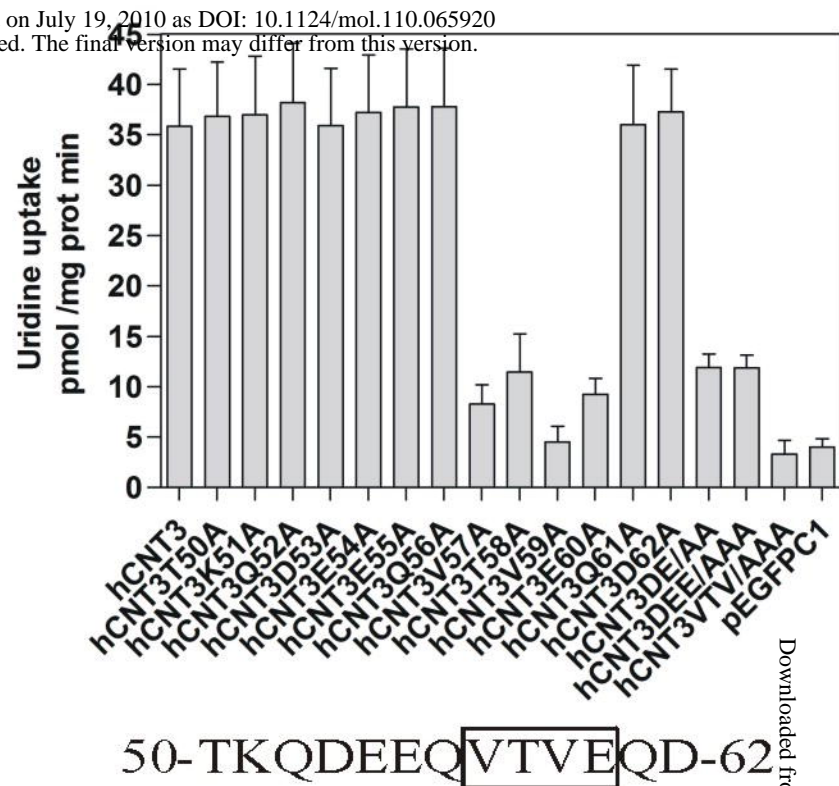
Figure 2

A)

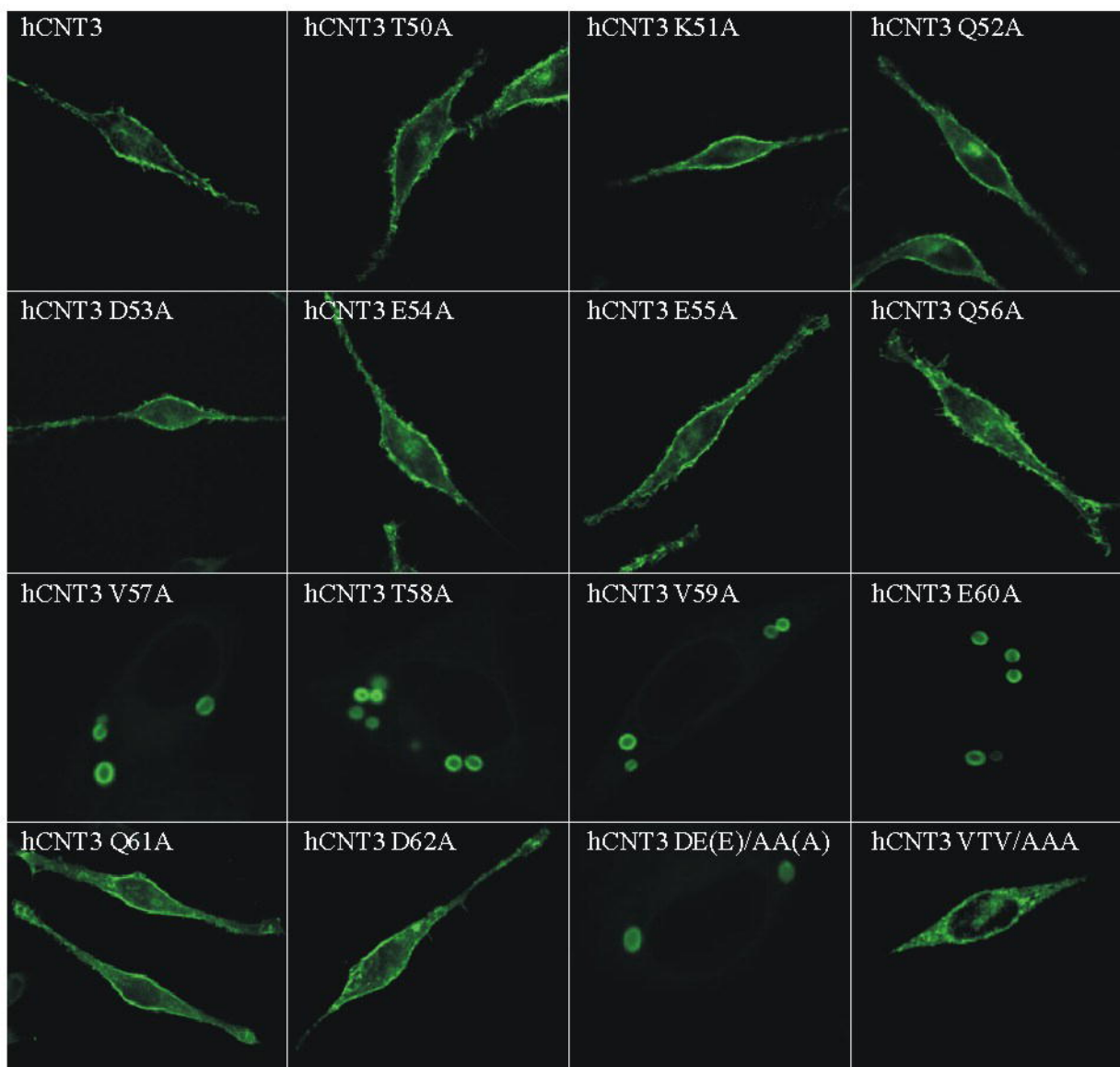
hCNT3  
ptCNT3  
goCNT3  
ppCNT3  
opCNT3  
pvCNT3  
miCNT3  
ogCNT3  
ttCNT3  
btCNT3  
stCNT3  
cpCNT3  
dnCNT3  
mCNT3  
rCNT3  
cfCNT3

TKQDEEQITVEQD
TKQDEEQVTVEQD
TKQDEEQVTVDQD
SKQDEEQVTIQDQD
AKQSEEQVTIEQD
TKQGEEQVTIEQD
TKQGEDHVTIERD
GKQGEEQVTIEQD
GKQVEEHITIGQD
TKQGEELVNIEQD
PKQGEEHITIEQD
AKQGEECITIEQD
AKQDDRQITIEQE
AKQDDRQITIEQE
AKQDEEQITIEQD

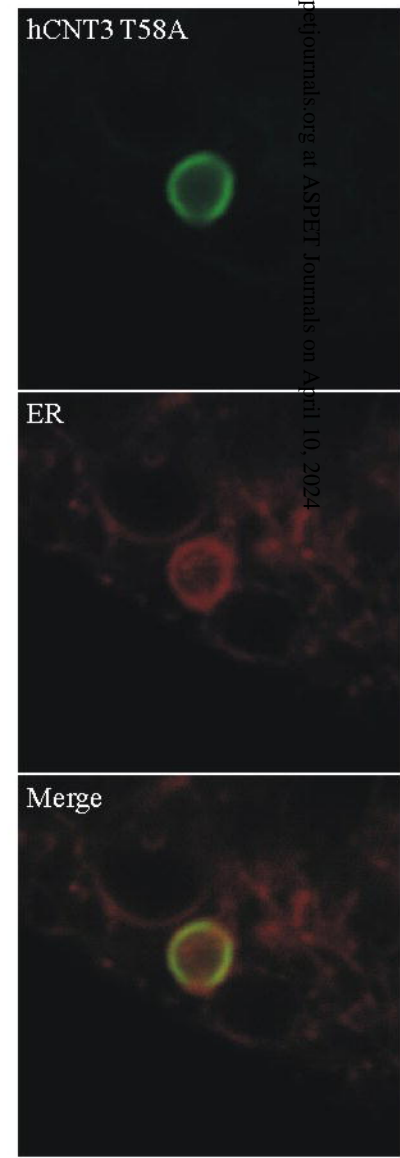
B)



C)



D)

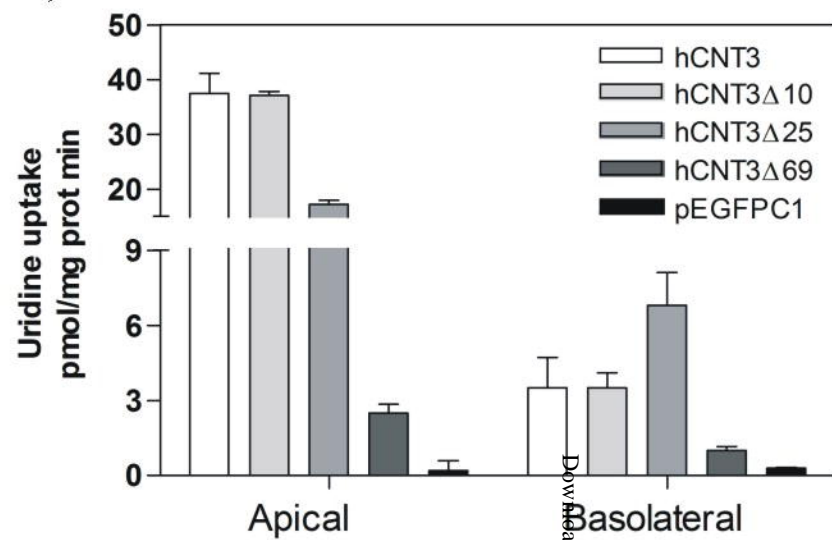




A)



B)



C)

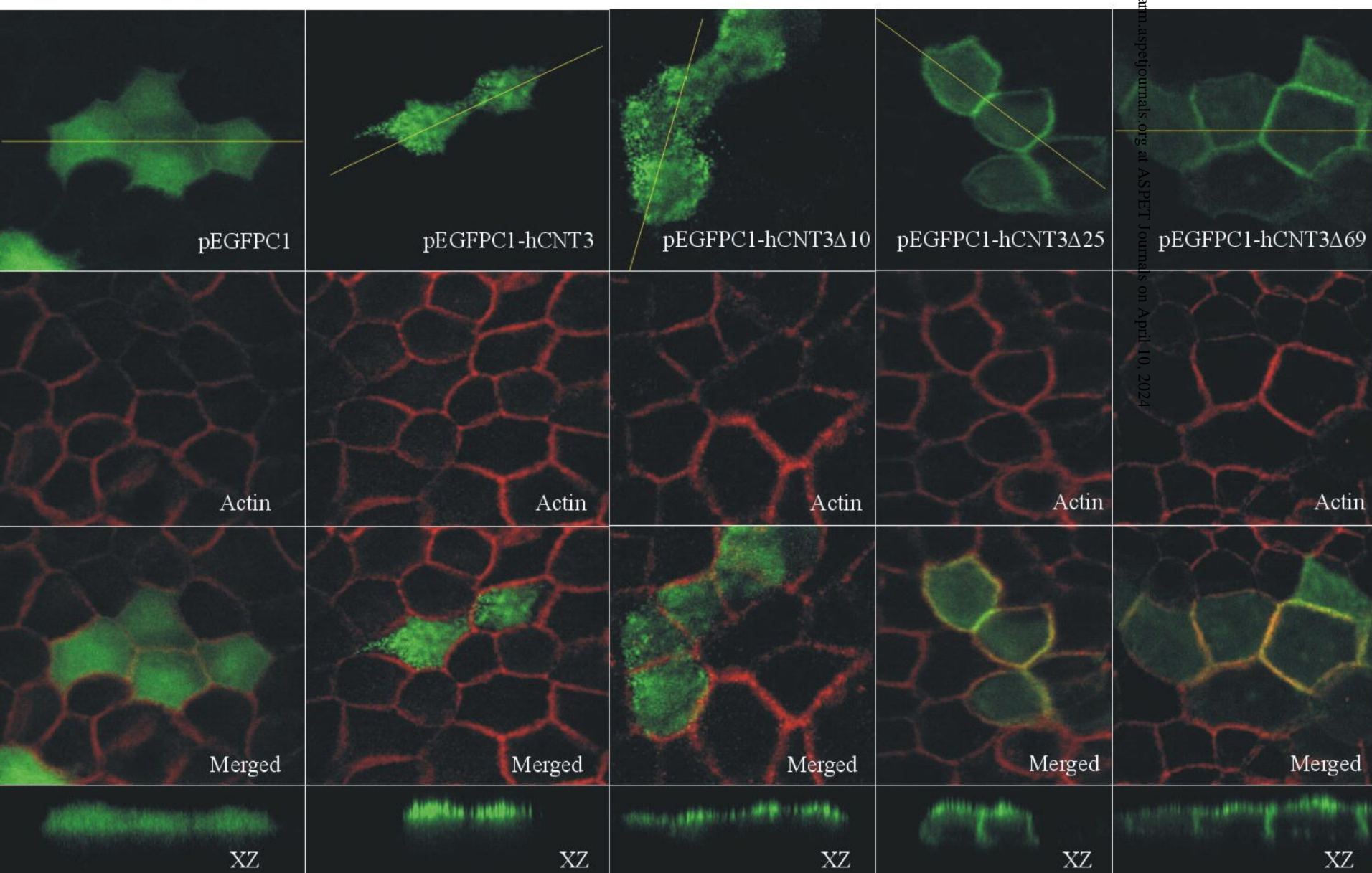


Figure 4

A) Molecular Pharmacology Fast Forward. Published on July 19, 2010 as DOI: 10.1124/mol.110.065920  
This article has not been copyedited and formatted. The final version may differ from this version.

hCNT3	AEGYSNVGFQNEENF
ptCNT3	AEGYSNVGFQNEENF
ppCNT3	AEGYSNTGFQNEENF
btCNT3	AQGCSNTGFQNDDEDG
cfCNT3	AEGCSNTGFQNDDEDL
ttCNT3	AEGCSNTGFQYDDDC
miCNT3	AQGCSNTGFQEEENC
pvCNT3	AEGYRNTGFQSEEDL
opCNT3	AEGFNNTAFQIEENF
stCNT3	TEGFSNTGFRNEELL
mCNT3	DLGRSNEAFQDEDL
rCNT3	DQGRLNEAFQDEDL

